Applied Catalysis A: General 489 (2015) 117–122

Contents lists available at ScienceDirect

Applied Catalysis A: General

journal homepage: www.elsevier.com/locate/apcata

Directing two azo-bridged covalent metalloporphyrinic polymers as highly efficient catalysts for selective oxidation

Weijie Zhang[a,*], Pingping Jiang[a,*], Ying Wang[a], Jian Zhang[b], Pingbo Zhang[a]

[a] The Key Laboratory of Food Colloids and Biotechnology, Ministry of Education, School of Chemical and Material Engineering, Jiangnan University, Wuxi 214122, China
[b] School of Chemistry and Environmental Science, Lanzhou City University, Lanzhou 730000, China

ARTICLE INFO

Article history:
Received 28 June 2014
Received in revised form 11 October 2014
Accepted 13 October 2014
Available online 23 October 2014

Keywords:
Covalent-organic polymer
Biomimetic catalysis
Selective oxidation
Porphyrin

ABSTRACT

Manganese meso-tetra (4-nitrophenyl)porphyrin (Mn-TNPP) with four nitro groups at periphery was employed as building moieties to condense with *p*-phenylenediamine and benzidine into extended π materials, respectively. Two covalent metalloporphyinic polymers (CMPs) linked by azo (—N═N—) were denoted as azo-CMP-1 and azo-CMP-2. FT-IR, XRD, SEM, TG, contact angle (CA) and XPS were used to analyze and characterize the synthesized heterogeneous materials. The catalytic study has demonstrated that azo-CMP catalysts displayed an excellent performance for epoxidation of olefins, especially cyclohexene. When azo-CMP-1 was recycled five times, its catalytic activity remained with an inconspicuous decrease. Additionally, azo-CMP series exhibited a amphipathic property evidenced by CA test, facilitating the diffusion of reactant into channels of azo-CMPs. Furthermore, the peak value of $Mn2p_{3/2}$ shifting to a higher value for azo-CMP-1 suggested that there was a catalysis-promoted electronic environment around the Mn(III) active sites, compared to either azo-CMP-2 or homogenous sites.

1. Introduction

Activation of unsaturated bonds is a subject of escalating interest in relation to the bio-inspired function mimicry of cyctochrome P450, as well as the development of highly active catalysts for selective oxidation reactions. Duplicating this impressive reactivity in synthetic systems has been the focus of intense research. In particular, metalloporphyrins is a well-established building blocks with catalytic active site to that of cyctochrome P450 and has been developed for various oxidation reactions [1–3].

However, the further development of metalloporphyrins as bio-catalyst in solution is still challenging, because of the recyclability drawback, formation of catalytically inactive dimers and inevitably fast degradation in homogeneous catalysis [4]. Nevertheless, several successful protocols have been formulated to circumvent these challenges. One such example involves immobilizing the porphyrins on insoluble supports, but this unavoidably dilutes the density of the active sites [5]. Another strategy decorates the porphyrin macrocycle with bulky functional groups to protect the active sites, which is limited by the difficulty of synthesizing these porphyrins [6]. Currently, an additional strategy that has spurred tremendous interest is to incorporate or encapsulate heme into various networks, including metal metalloporphyrins-organic frameworks (MMOFs) [7–13], covalent metalloporphyrinic frameworks (CMFs) [14–17] and covalent metalloporphyrinic polymers (CMPs) [18–22]. Among them, covalent metalloporphyrinic polymers (CMPs) are the easiest to design and develop among the three aforementioned classes of materials, they are non-crystalline and have non-uniform pores that are typically somewhat ill-defined. Therefore, there is an urgent need to develop novel CMPs to target highly efficient bio-catalysts.

In fact, covalent organic polymers have been intentionally fabricated since at least the early 1960s by incorporating functional monomers into polymerization processes, yielding three-dimensional (3D)-network materials [20,23]. Recent researches focus on assembling novel linkages with light element composition, rigid nature and discrete bonding direction of arenes in order to make aromatic π systems [24–27]. This has potential to provide a desirable platform for the design and development of CMP materials as promising heterogeneous bio-catalysts.

From the point view of catalysis, the CMP with accessibility of the open channels, can be considered as self-supported catalysts with an enhanced performance due to their high-density active sites into network. The tetrapyrrolic macrocycles of porphyrins play an important role in the design of extended supramolecular

* Corresponding authors. Tel.: +86 510 85913617; fax: +86 13506196132.
E-mail addresses: fengyunzwj@126.com (W. Zhang), ppjiang@jiangnan.edu.cn (P. Jiang).

http://dx.doi.org/10.1016/j.apcata.2014.10.023
0926-860X/

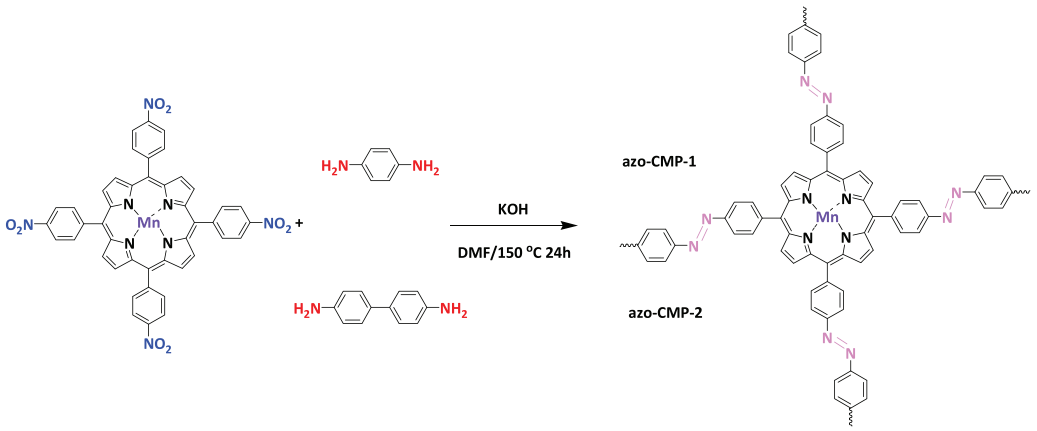

Fig. 1. Syntheses of two azo-CMPs. Green powders of azo-CMPs were obtained by reacting manganese meso-tetra (4-nitrophenyl)porphyrin, with two aromatic amines, namely *p*-phenylenediamine (azo-CMP-1) and benzidine (azo-CMP-2) in DMF at 150 °C in the presence of potassium hydroxide under an atmosphere of N_2.

lattices, which derives from their robust structure, remarkable thermal and oxidative stability, and unique catalytic properties. More importantly, the heterogeneous nature of CMPs can be very useful to separate the catalyst from the products of interest, recover it after simple filtration procedures and finally regenerate it for successive catalytic runs. Therefore, this motivates us to target efficient heterogeneous catalysts with open coordination frameworks through novel linkage, which is essential to catalysis application.

With this background in mind, we reported the development of new CMPs based on the azo (—N=N—) linkage that exhibited high performance on selective oxidation (Fig. 1). Accordingly, we employed manganese meso-tetra (4-nitrophenyl)porphyrin (Fig. 1, Mn-TNPP) with four nitro groups at periphery as amino component to condense with nitro, in order to demonstrate the feasibility of the strategy and features of various CMP catalysts. Catalytic study has demonstrated that azo-CMP-1 and azo-CMP-2 can catalyze the epoxidation of a variety of natural substrates, acting as an effective peroxidase mimic. The reported azo linkage not only stabilizes the catalytic sites by hindering it from forming catalytically inactive dimers, but also endows the catalysts a rare amphipathic property which facilitates the diffusion of reactants, together with a catalysis-promoted electronic environment evidenced by XPS study.

2. Experimental

2.1. Manganese meso-tetra (4-nitrophenyl)porphyrin (Mn-TNPP)

The compound TNPP was prepared by the method described in the literature as follows [28]. 4-Nitrobenzaldehyde (22.0 g, 1.45×10^{-1} mol) and acetic anhydride (24.0 mL, 2.54×10^{-1} mol) was dissolved in propionic acid (600 mL). The solution was then refluxed, to which pyrrole (10.0 mL, 1.44×10^{-1} mol) was slowly added. After refluxing for 30 min, the resulting mixture was cooled to give a precipitate which was collected by filtration, washed with H_2O and methanol, and dried under vacuum. The resulting powder was dissolved in pyridine (160 mL) which was refluxed for 1 h. After cooling, the precipitate was collected by filtration and washed with methanol to give 5,10,15,20-tetrakis(4-nitrophenyl)-21*H*,23*H*-porphyrin as a purple powder in 14% yield. Mn-TNPP was synthesized after a metallization process of TNPP with $MnCl_2$ in DMF [29,30].

2.2. Synthesis of azo-CMP-1

Mn-TNPP (0.25 g, 0.3 mmol) and *p*-phenylenediamine (0.065 g, 0.6 mmol) were dissolved in DMF (19 mL) in a three-necked round bottom flask equipped with a condenser, thermocouple and magnetic stirrer. KOH (0.16 g, 2.86 mmol) was added to this solution while stirring. The temperature of the reaction mixture was increased slowly up to 150 °C with vigorous stirring under N_2 atmosphere and stirred at this temperature for 24 h. The reaction mixture was cooled to room temperature, added to 80 mL of distilled H_2O and stirred for 1 h. Green precipitate was filtered off, immersed in DMF for 1 day and then washed with warm distilled H_2O (×5), Me_2CO (×5) and THF (×5). Subsequently, green precipitates were dried at 150 °C under vacuum for 8 h to yield azo-CMP-1 (0.18 g) in 57% yield.

2.3. Synthesis of azo-CMP-2

Mn-TNPP (0.339 g, 0.4 mmol) and benzidine (0.147 g, 0.8 mmol) were dissolved in DMF (25 mL) in a three-necked round bottom flask equipped with a condenser, thermocouple and magnetic stirrer. KOH (0.22 g, 3.92 mmol) was added to this solution while stirring. The catalyst amount in DMF solution was about 0.15 mmol of KOH/mL DMF for both synthesis. The temperature of the reaction mixture was increased slowly up to 150 °C with vigorous stirring under N_2 atmosphere and stirred at this temperature for 24 h. The reaction mixture was cooled to room temperature, added to 100 mL of distilled H_2O and stirred for 1 h. Green precipitate was filtered off, immersed in DMF for 1 day and washed with warm distilled H_2O (×5), Me_2CO (×5) and THF (×5). Subsequently, green precipitates were dried at 150 °C under vacuum for 8 h to yield azo-CMP-2 (0.16 g) in 33% yield.

2.4. Measurement of catalytic performance

All of the reactions were carried out at desired temperature under air in a 50 mL flask equipped with a magnetic stirrer bar. Olefin (500 mM), TBHP (1000 mM), catalyst (0.01 mmol, 5 mM), acetonitrile (3.0 mL) sealed and bromobenzene as internal standard in a Teflon-lined screwcap vial were stirred at 70 °C for 24 h. The progress of reaction was monitored by GC–MS. The catalyst was thoroughly washed with EtOH and hot water before reuse. The sample was taken from the supernatant after centrifugation. The injector and detector temperature was both set at 260 °C in order to test all the products (TPD: 50 °C for 1 min, then 10 °C min^{-1} up to 140 °C and 140 °C for 15 min). GC was analyzed on a HP 6890 series GC system, and MS on a 5971A Mass selective Detector.

2.5. Characterization of catalysts

The IR spectra were recorded on an ABB Bomem FTLA2000-104 spectrometer. X-ray power spectra were recorded using a bruker

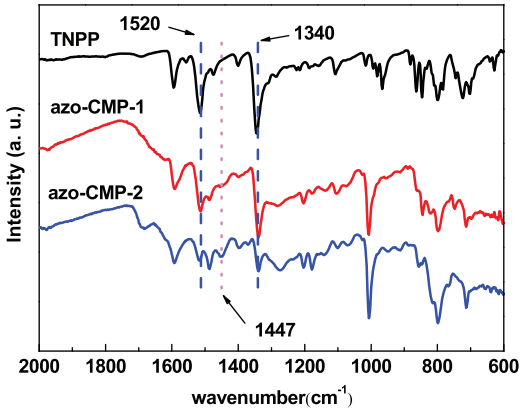

Fig. 2. FT-IR spectra of: TNPP (black line), azo-CMP-1 (red line), azo-CMP-2 (blue line). (For interpretation of the references to color in this figure legend, the reader is referred to the web version of this article.)

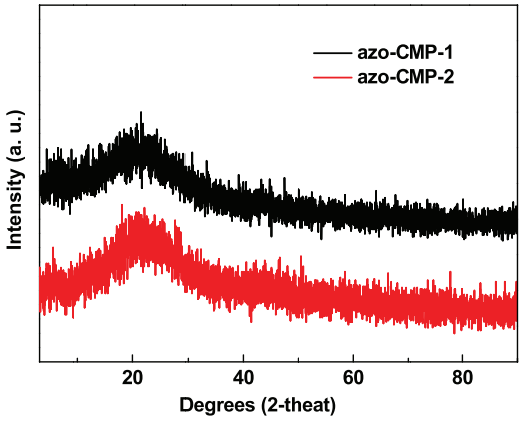

Fig. 3. Wide-angle XRD patterns of azo-CMP-1 (black line), azo-CMP-2 (red line). (For interpretation of the references to color in this figure legend, the reader is referred to the web version of this article.)

D8-Advance diffractometer with Cu-*K*α radiation. TG of the samples was recorded using a Mettler TGA/SDTA 851 E analyzer in the temperature range 50–800 °C at a heating rate of 20 °C/min. SEM measurements were performed on a CamScan CS44 scanning electron microscope. The samples for TEM observation were suspended in ethanol and supported on carbon-coated copper. X-ray photoelectron spectroscopy (XPS) was recorded by a Kratos Ultra DLD imaging spectrometer (UK) using an Al *K*α Rradiation (1486.6 eV) in East China University of Science and Technology. The powdered samples were pressed into pellets prior to the XPS studies.

3. Results and discussion

3.1. Characterization of catalysts

The structures of synthesized compounds (azo-CMP-1 and azo-CMP-2) were characterized in Fig. 2, in order to monitor the variations in the functional groups. The characteristic stretching band for —N=N— functionality in the FT-IR spectrum was clearly visible at 1447 cm^{-1} along with the respective bands for aromatic rings [31]. Additionally, the FT-IR bands located at 1520 and 1340 cm^{-1} correspond to N—O stretching mode, suggesting the presence of unreacted terminal nitro groups.

Powder XRD analysis of these azo-CMPs revealed no strong diffraction peaks (Fig. 3), implying that the micro-porous polymers were composed of an amorphous network. It is pertinent to mention that using pre-synthesized metalloporphyrins building blocks for CMP formation also resulted in materials without any definite XRD pattern of monomeric units.

Most recently, a research showed that if the active centers can be neatly arranged to form a graphene-like 2D porous covalent organic framework, then this may provide an ideal system both to enhance the catalytic activity and to protect the active centers [14]. Field-emission scanning electron microscopy (SEM) images show that azo-CMP-1 was composed of agglomerated plate-shaped particles (Fig. 4). However, the SEM image showed that the azo-CMP-2 material was composed of coralline-shaped particles with smaller size. As expected, the longer length of linker for azo-CMP-2, led to a significant distortion during the growth of azo-CMP-2. Consequently, the azo-CMP-1 heterostructure, favoring π–π stacking in aggregates, would demonstrate a better performance in biomimetic catalytic reactions, presumably due to its graphene-like morphology. Figs. 3 and 4 were results not shown in the bibliography.

To elucidate the thermal stability of —N=N— bond, TG/DTG analysis of azo-CMP-1 and azo-CMP-2 was determined and shown in Fig. 5. The comparison of azo-CMP-1 and azo-CMP-2 reported in this work showed that they had almost similar decomposition profiles. However, azo-CMP-1 was stable up to 346 °C, possessing a better thermal stability than azo-CMP-2 (340 °C).

3.2. Catalytic activity

To compare the efficiency of different catalysts, described above, styrene was used as a model substrate. The kinetic profiles for the selective oxidation of styrene were represented in Fig. 6. It can clearly be seen that azo-CMP-1 as catalyst displayed a better performance than azo-CMP-2. We also noticed that the comparably low conversion of styrene epoxides was related with the low electron density of double bond, which usually reduced

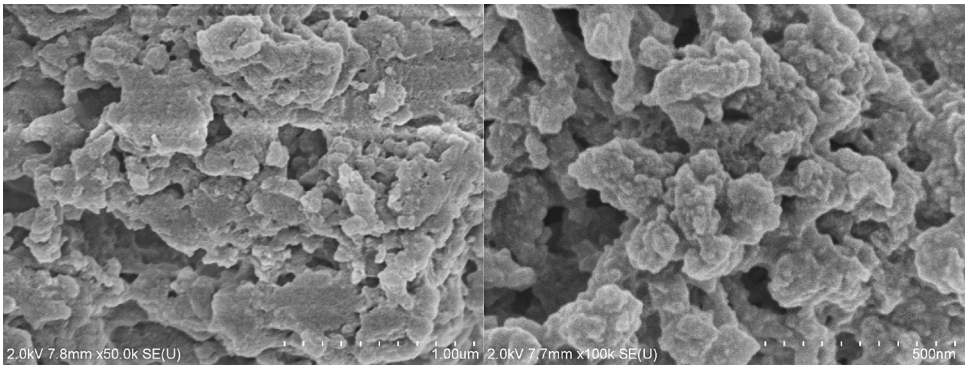

Fig. 4. SEM and TEM images of sample azo-CMP-1 (left) and azo-CMP-2 (right).

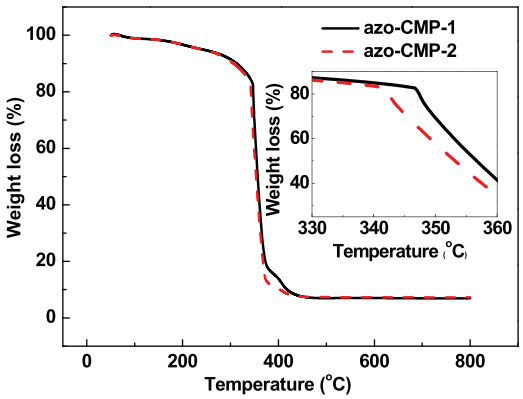

Fig. 5. TG/DTG curves for sample azo-CMP-1 (left) and azo-CMP-2 (right).

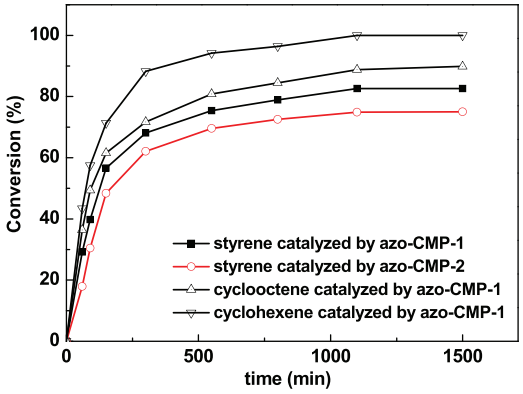

Fig. 6. Plot of conversion *versus* time with different substrates and catalysts.

their nucleophilicity toward electrophilic oxygen of catalytic intermediate-porphyrin-Mn(V)═O [30].

The catalytic activity of cyclohexene showed a higher conversion than cyclooctene. The steric hindrance should be attributed to this result. The size of cyclohexene was smaller than cyclooctene. Consequently, it was hard for cyclooctene to be accessible to active sites. Moreover, we also viewed recent published works about epoxidation of cyclohexene and cyclooctene by metal metalloporphyrinic framework catalyst, the results showed that the conversion of cyclohexene was higher than that of cyclooctene [10,32]. Although the cyclohexene was usually considered in the bibliography as more difficult to oxidized than cyclooctene, the rigorous dimension of channel size within catalyst has become the main factor that affects the conversion of substrate with similar structure. This observation highlighted that azo-CMP-1 offered channels with accessible catalytic sites for the substrates, which greatly facilitated their diffusion.

To further confirm aforementioned claim, we compared the catalytic activities of azo-CMP-1 with their molecular components of $MnCl_2$ and Mn-TNPP shown in Table 1. $MnCl_2$ showed a lower catalytic activity with conversions of 57%. In comparison, Mn-TNPP did show quite moderate catalytic activity that could transform 86% of the cyclohexene into the cyclohexene oxide, but still were not as efficient as heterogeneous azo-CMP-1 (100% conversion). In order to understand the steric effect on catalytic efficiency, a range of natural alkenes were selected to be oxidized in this catalytic system, including linear alkenes, styrene and *trans*-stilbene. Overall, increasing the steric size of alkenes triggered lower catalytic activity.

From the catalytic results, it was obvious that the conversion of cyclic olefin was higher than the linear olefin. With this regard, we began to address this from two points: the position of double-bond in olefins and the contact between catalyst and substrate. On one hand, the conversions depend on the position and steric configuration of the double bond, as a result of steric effects during the epoxidation. On the other hand, the conversions are decreased by increasing the chain length or the cross-section of the olefin (1-hexene > cyclohexene). Furthermore, as the length of linear olefin increases, the mobility of alkene decreases, and therefore, the accessibility of active site will be difficult for 1-octane and 1-dodecene.

The excellent heterogeneous catalysts should not only have high catalytic activity and selectivity, but should also be structurally stable and thus be easily recovered for continuous usage. Compound azo-CMP-1 can be simply recycled by filtration, which was subsequently reused in successive runs. The recycled azo-CMP-1 still exhibited a very high conversion of 97% and selectivity of >99% when cyclohexene being used as substrate, thus indicating that azo-CMP-1 was indeed a heterogeneous catalyst for cyclohexene epoxidation. The average turnover frequency (TOF) in the first 12 h was also listed in Table 1.

With the aim at excluding any possible contamination by homogeneous metal active sites responsible for observed catalyst activity and selectivity, a hot filtration test in azo-CMP-1 have been performed shown in Fig. 7. Accordingly, the oxidation was allowed to proceed for 90 min before being split into two fractions, one containing the suspended catalyst and the other being filtered to remove any solid precipitate. The former solution was kept to react with additional azo-CMP-1 catalyst. For the latter one, the catalyst was separated and discarded form the reaction mixture. Then, the supernatant was analyzed by GC test. Finally, the conversion of first fraction did well with the result of solution containing catalyst all through. And, the catalytic performance of latter oxidation increased slightly. Altogether, this hot filtration test confirmed a truly heterogeneous process.

Some benchmarking of azo-CMP-1 has been carried out by comparison with well known and readily available catalysts. Table 2 contains the epoxidation of *trans*-stilbene studies in the previous literature. Based on the performance of azo-CMP-1 and homogenous catalysts toward the *trans*-stilbene epoxidation, azo-CMP-1 outperformed the 2D layered in epoxidation *via* its structural resistance to formation of catalytically inactive species.

3.3. Catalytic behavior study

Although the successive catalytic runs (Table 1, entry 2) and comparison with ever reported catalysts (Table 2) have evidenced that CMP strategy could prevent the self-dimerization of porphyrin centers by bimolecular interaction to form the M-O-O-M unit [35,4], porphyrinic networks constructed *via* Yamamoto homocoupling reaction usually exhibit strong hydrophobicity with a water contact angle about 135° [36]. This property greatly increases the diffusion resistance by restricting exposing catalytically active sites to those reactants with hydrophilic properties. However, if there was no hydrophobic properties, the by-product of TBHP-tertiary butanol in epoxidation would coordinate with Mn sites. Therefore, a moderate hydrophobic property should facilitate the catalytic application. Interestingly, —N═N— bond endowed the porphyrinic polymers (azo-CMP-1 and azo-CMP-2) with a rare amphipathic property (Fig. 8). Thus, we supposed that azo-CMPs catalysts could provide a desirable micro-environment for selective oxidation, facilitating the spread of reactants and accordingly enhancing the overall catalytic performance.

Although the graphene-like morphology of azo-CMP-1 could interpret its superior catalytic activity to azo-CMP-2, the nature of Mn sites in azo-CMPs has not been revealed. To identify this point, XPS analysis can help to reveal the oxidant state of Mn sites of molecules in azo-CMPs. As shown in Fig. 9, one may notice that the

Table 1
Scope of azo-CMPs catalyzed epoxidation of alkenes[a].

Entry	Substrate	Catalyst	Conversion (%)[b]	Selectivity (%)[c]	TOF[h]
1		azo-CMP-1	79	>99	6.6
2		azo-CMP-1	100/97[d]	>99	8.3
3		azo-CMP-1	58	>99	4.8
4	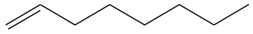	azo-CMP-1	35	>99	2.9
5	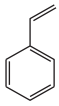	azo-CMP-1	82	68[e]	4.6
6	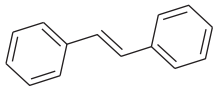	azo-CMP-1	31	50[f]	1.3
7	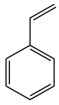	azo-CMP-2	69	65[e]	5.7
8		$MnCl_2$	57	78[g]	3.7
9		Mn-TNPP	86	53[g]	3.8

[a] Olefin (500 mM), TBHP (1000 mM), catalyst (0.01 mmol, 5 mM), acetonitrile (3.0 mL) sealed and bromobenzene as internal standard in a Teflon-lined screwcap vial were stirred at 70 °C for 24 h.
[b] Conversion [%].
[c] Selectivity [%] were determined by GC using an SE-54 column (50 °C for 1 min, then 10 °C min^{-1} up to 140 °C and 140 °C for 15 min).
[d] After fifth cycles.
[e] Benzaldehyde and phenylacetaldehyde.
[f] Benzaldehyde.
[g] 2-Cyclohexene-1-ol and 2-cyclohexene-1-one.
[h] The TOF was defined as mmol of product per mmol of catalyst per hour.

peak value of $Mn2p_{3/2}$ shifted to a higher value (642.6 eV for azo-CMP-1) compared to the binding energy of Mn(III) in azo-CMP-2 (642.3 eV). In a previous study, the reported 642.2 eV of Mn-TPP also was close to the $Mn2p_{3/2}$ value of azo-CMPs [30,33,37–39]. While, the peak value of $Mn2p_{3/2}$ for azo-CMP-1 and azo-CMP-2 both shifted to higher value, relative to Mn-TPP. Then, it can be concluded that the redox property of the Mn complexes was changed after being assembled into extended π systems, that is, a charge transfer was induced from Mn(III) center to linkers, especially for azo-CMP-1. Therefore, the catalytic ability of Mn(III) center in azo-CMPs can be greatly enhanced due to such a desirable catalysis-promoted electronic environment.

Interestingly, there was a satellite peak at 654.2 and 653.4 eV, respectively, beside the main peak of $Mn2p_{3/2}$ in azo-CMPs. The resulting satellite peak could be attributed to the manganese-oxo species from catalyst. Furthermore, the Mn sites of azo-CMP series were easily activated. Hence, our reported azo-CMP series had a strongly biomimetic characteristic.

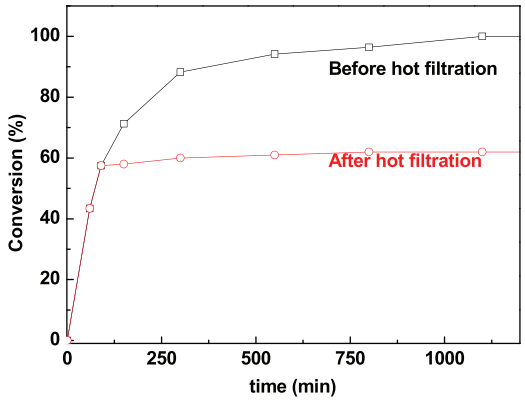

Fig. 7. Conversion of cyclohexene into epoxide based on a hot filtration test.

Table 2
Catalytic activities toward the homogenous oxidation of *trans*-stilbene of some previously reported catalyst.

Catalyst	Conversion (%)	Yield (%)	TOF
This work	31	15	1.3
MMPF-3 [11]	96	58	69
PPF-1Co [11]	24	7	15
MMPF-5(Co) [12]	87	71	59
MMPF-5 [12]	9	5	4.2
Fe(TMP)Cl [33]	Trace	Trace	0
Au/TiO_2 [34]	95	71	3.0

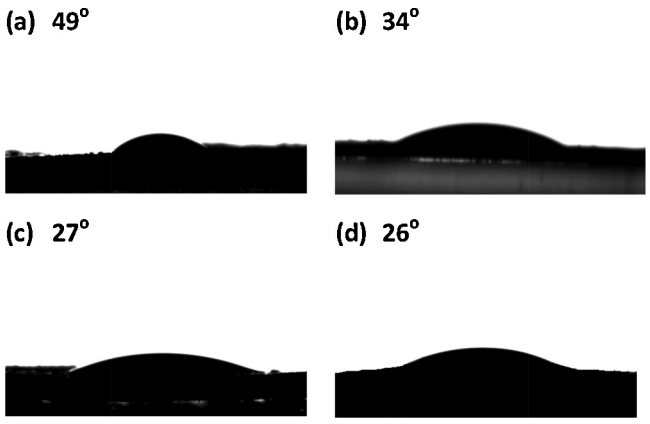

Fig. 8. Contact angle for a droplet of (a) water on azo-CMP-1, (b) water on azo-CMP-2, (c) oil on azo-CMP-1 and (d) oil on azo-CMP-2.

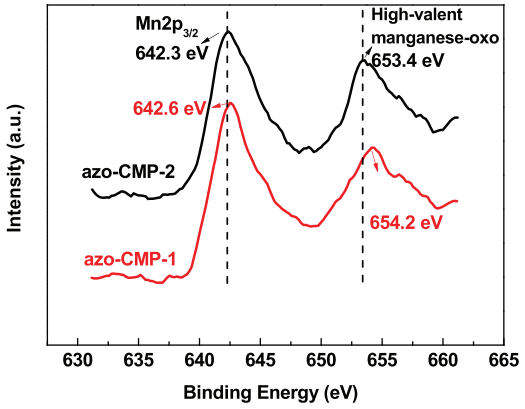

Fig. 9. XPS spectra for the clean azo-CMPs surface, Mn 2p region.

4. Conclusions

Two efficient catalysts azo-CMP-1 and azo-CMP-2 were successfully constructed with meso-tetra (4-nitrophenyl)porphyrin as building blocks *via* azo (—N=N—) linkage. An excellent performance with 100% conversion and no less than 99% selectivity for cyclohexene was obtained, when azo-CMP-1 was employed as catalyst. On the other hand, various of other unsaturated olefins with different steric sizes were investigated to confirm the catalytically active sites being located into the channels of catalysts. Contact angle research showed that azo linkage endowed azo-CMPs with a rare amphipathic property, which was essential to the reactant diffusion during the catalytic process. The SEM photos together with XPS study, both evidenced azo-CMP-1 with a superior catalytic activity, with respect to azo-CMP-2. Therefore, our reported strategy assembling metalloporphyrins into extended π materials linked by azo bonds, provided a promising platform to design functional polymers as catalysts in selective oxidation.

Acknowledgments

Special thanks to Dr. Liu from East China University of Science and Technology for his help on testing of XPS data. This work was supported financially by the National "Twelfth Five-Year" Plan for Science & Technology (2012BAD32B03), the National Natural Science Foundation of China (20903048) and the Innovation Foundation in Jiangsu Province of China (BY2013015-10).

References

[1] M. Zhao, S. Ou, C.D. Wu, Acc. Chem. Res. 47 (2014) 1199–1207.
[2] M. Costas, Coord. Chem. Rev. 255 (2011) 2912–2932.
[3] P.R. Ortiz de Montellano, Chem. Rev. 110 (2010) 932–948.
[4] T.C. Bruice, Acc. Chem. Res. 24 (1991) 243–249.
[5] T. Xue, S. Jiang, Y. Qu, Q. Su, R. Cheng, S. Dubin, C.-Y. Chiu, R. Kaner, Y. Huang, X. Duan, Angew. Chem. Int. Ed. 51 (2012) 3822–3825.
[6] M. Shema-Mizrachi, G.M. Pavan, E. Levin, A. Danani, N.G. Lemcoff, J. Am. Chem. Soc. 133 (2011) 14359–14367.
[7] M.H. Xie, X.L. Yang, C.D. Wu, Chem. Commun. 47 (2011) 5521–5523.
[8] M.H. Xie, X.L. Yang, Y. He, J. Zhang, B. Chen, C.D. Wu, Chem. Eur. J. 19 (2013) 14316–14321.
[9] X.L. Yang, C. Zou, Y. He, M. Zhao, B. Chen, S. Xiang, M. O'Keeffe, C.D. Wu, Chem. Eur. J. 20 (2014) 1447–1452.
[10] C. Zou, T. Zhang, M.H. Xie, L. Yan, G.Q. Kong, X.L. Yang, A. Ma, C.D. Wu, Inorg. Chem. 52 (2013) 3620–3626.
[11] L. Meng, Q. Cheng, C. Kim, W.Y. Gao, L. Wojtas, Y.S. Chen, M.J. Zaworotko, X.P. Zhang, S. Ma, Angew. Chem. Int. Ed. 51 (2012) 10082–10085.
[12] X.-S. Wang, M. Chrzanowski, L. Wojtas, Y.-S. Chen, S. Ma, Chem. Eur. J. 19 (2013) 3297–3301.
[13] B. Li, Y. Zhang, D. Ma, T. Ma, Z. Shi, S. Ma, J. Am. Chem. Soc. 136 (2014) 1202–1205.
[14] X.-S. Wang, M. Chrzanowski, D. Yuan, B.S. Sweeting, S. Ma, Chem. Mater. 26 (2014) 1639–1644.
[15] X. Feng, L. Chen, Y. Dong, D. Jiang, Chem. Commun. 47 (2011) 1979–1981.
[16] S. Kandambeth, D.B. Shinde, M.K. Panda, B. Lukose, T. Heine, R. Banerjee, Angew. Chem. Int. Ed. 52 (2013) 13052–13056.
[17] L. Chen, Y. Yang, Z. Guo, D. Jiang, Adv. Mater. 23 (2011) 3149–3154.
[18] P.M. Budd, B. Ghanem, K. Msayib, N.B. McKeown, C. Tattershall, J. Mater. Chem. 13 (2003) 2721–2726.
[19] R.K. Totten, Y.S. Kim, M.H. Weston, O.K. Farha, J.T. Hupp, S.T. Nguyen, J. Am. Chem. Soc. 135 (2013) 11720–11723.
[20] P. Kaur, J.T. Hupp, S.T. Nguyen, ACS Catal. 1 (2011) 819–835.
[21] H. Ma, H. Ren, S. Meng, F. Sun, G. Zhu, Sci. Rep. 3 (2013) 2611.
[22] A.M. Shultz, O.K. Farha, J.T. Hupp, S.T. Nguyen, Chem. Sci. 2 (2011) 686–689.
[23] O.L. Hollis, Anal. Chem. 38 (1966) 309–316.
[24] H.A. Patel, S.H. Je, J. Park, Y. Jung, A. Coskun, C.T. Yavuz, Chem. Eur. J. 20 (2014) 772–780.
[25] H.A. Patel, S.H. Je, J. Park, D.P. Chen, Y. Jung, C.T. Yavuz, A. Coskun, Nat. Commun. 4 (2013) 1357–1364.
[26] S. Braese, T. Muller, RSC Adv. 4 (2013) 6886–6907.
[27] L. Li, H. Zhao, J. Wang, R. Wang, ACS Nano 8 (2014) 5352–5364.
[28] M. Yuasa, K. Oyaizu, A. Yamaguchi, M. Kuwakado, J. Am. Chem. Soc. 126 (2004) 11128–11129.
[29] A.D. Adler, J. Inorg. Nucl. Chem. 32 (1970) 2443–2445.
[30] W. Zhang, P. Jiang, Y. Wang, J. Zhang, J. Zheng, P. Zhang, Chem. Eng. J. 257 (2014) 28–35.
[31] L.M. Sáiz, P.A. Oyanguren, M.J. Galante, React. Funct. Polym. 72 (2012) 478–485.
[32] X.L. Yang, C.D. Wu, Inorg. Chem. 53 (2014) 4797–4799.
[33] W. Nam, J. Inorg. Biochem. 80 (2000) 219–225.
[34] P. Lignier, F. Morfin, S. Mangematin, L. Massin, J.L. Rousset, V. Caps, Chem. Commun. (2007) 186–188.
[35] C.G. Bezzu, M. Helliwell, J.E. Warren, D.R. Allan, N.B. McKeown, Science 327 (2010) 1627–1630.
[36] X.S. Wang, J. Liu, J.M. Bonefont, D.Q. Yuan, P.K. Thallapally, S. Ma, Chem. Commun. 49 (2013) 1533–1535.
[37] J. Xie, Y.J. Wang, Y. Wei, Catal. Commun. 11 (2009) 110–113.
[38] B.E. Murphy, S.A. Krasnikov, N.N. Sergeeva, A.A. Cafolla, A.B. Preobrajenski, A.N. Chaika, O. Lubben, I.V. Shvets, ACS Nano 8 (2014) 5190–5198.
[39] A. Kaplan, E. Korin, A. Bettelheim, Eur. J. Inorg. Chem. 2014 (2014) 2288–2295.